ISSN 2070-2051, Protection of Metals and Physical Chemistry of Surfaces, 2019, Vol. 55, No. 3, pp. 527–534. © Pleiades Publishing, Ltd., 2019.

NEW SUBSTANCES, MATERIALS, AND COATINGS

Friction and Wear Behavior of Multilayer $[Al/AlN]_n$ Coatings Deposited on AISI52100 Steel

Eduardo Alfaro-Pérez[a], Fernando Chiñas-Castillo[a,*], Francisco J. Flores-Ruiz[b], Rafael Alavez-Ramirez[c], Magdaleno Caballero-Caballero[c], and Javier Lara-Romero[d]

[a] *Department of Mechanical Engineering, Tecnológico Nacional de México/Instituto Tecnológico de Oaxaca, Calz. Tecnológico # 125, Oaxaca, Oax., C.P. 68030 México*

[b] *CONACYT-Instituto de Física, Benemérita Universidad Autónoma de Puebla, Apdo. Post. J-48, Puebla, Pue. 72570 México*

[c] *Instituto Politécnico Nacional, CIIDIR Unidad Oaxaca, Oaxaca, Oax., México*

[d] *Department of Chemical Engineering, Universidad Michoacana de San Nicolas de Hidalgo, Morelia, Mich., Mexico*

**e-mail: fernandochinas@gmail.com*

Received July 8, 2017; revised December 11, 2017; accepted January 9, 2018

Abstract—In this study, a set of multilayer hard nanocrystalline coatings of Al/AlN with 35, 55 and 75 bilayer were prepared by DC magnetron sputtering on AISI 52100 steel specimens at nitrogen fractions of 35 and 65% in the Ar + N_2 discharge. X-ray diffraction analysis indicates a polycrystalline structure of AlN + Al and AlN phases for 35% N_2 and 65% N_2 fraction, respectively. Nanoindentation tests showed hardness values from 11 to 19 GPa and elastic modulus of ~200 GPa almost independent of the bilayer number for both, 35% N_2 and 65% N_2. Tribological tests evaluated with a CSM pin-on-disk tribometer showed a reduction in the wear rate compared to AISI 52100 steel specimens. Multilayer coatings deposited at 35% N_2 fraction presented a lower friction coefficient than those coatings deposited at 65% N_2. The origin of such a decrease in the coefficient of friction was associated with the presence of the Al phase in the coatings deposited at 35% N_2. The wear mechanism for both 35 and 65% N_2 were different. For the first case, the wear is controlled by plastic flow and abrasive wear, while in the second case, is dominated by adhesive wear.

Keywords: sputtering, multilayer, nanocrystalline, Al/AlN, tribological

DOI: 10.1134/S207020511903002X

1 INTRODUCTION

Hard and super hard coatings are new technological advances. Nowadays their use is present in many different applications, from industrial tools to electronic devices, mechanical elements or aerospace applications. Hard coatings made of aluminum nitride have been used to protect against corrosion and extend life of machine elements, improving their performance and quality. Deposition of these coatings on solid surfaces has been performed by ion beam reactive sputtering [1], reactive evaporation [2], chemical vapor deposition [3, 4], molecular beam epitaxy [5–7], and others. Reactive sputtering has an additional advantage over the others in that it can produce highly dense coatings at low substrate temperature. Deposition control parameters allow a wide range of properties for different applications such as electronic, optic, data storage, decoration [8].

In the last two decades, hard coatings based on nitrides such as TiN, CrN captured attention because of their high hardness, stable friction performance, and good wear resistance [9, 10]. A further reason is because multilayer metal/ceramic coatings in nanoscale have the possibility of reaching very high hardnesses [11–13]. Aluminum is a material well known for its excellent ductility and low density while aluminum nitride can be used in mechanical and more recently for tribological purposes, although its behavior in this last application is not well understood up to now. There are only a few tribological studies reported on the literature about AlN coatings despite that they are necessary requirements because the coating has to withstand the operating stresses generated by the contact pressures in machine elements. Zhang et al. [14, 15] carried out friction and wear studies of reciprocating motion on a ball-on-disk micro-tribometer UMT employing GCr15 steel balls against the Al/AlN multilayer samples prepared by DC sputtering and deposited on silicon substrate at 2–24 nm thick modulation periods. The authors reported higher wear resistance and lower friction coefficients for the multilayer Al/AlN (14 nm thick) coated specimens. Subramanian et al. [16] deposited AlN monolayer coatings with hexagonal wurtzite structure and 2 micron thick on mild steel substrates. These coatings showed better friction and wear performance than the substrate on a

Table 1. Thickness and r.m.s. roughness of the multilayer $[Al/Al{-}N]_n$ coatings

Sample	Thickness, μm	r.m.s. roughness, nm
$[Al/Al{-}N]_{35}$@35%N_2	0.80	7.40
$[Al/Al{-}N]_{55}$@35%N_2	1.70	7.50
$[Al/Al{-}N]_{75}$@35%N_2	1.50	11.20
$[Al/Al{-}N]_{35}$@65%N_2	0.60	8.80
$[Al/Al{-}N]_{55}$@65%N_2	1.02	4.20
$[Al/Al{-}N]_{75}$@65%N_2	1.30	5.00
Substrates	—	8.00

block on ring system. Yang et al. [17] tested (1 0 3)-oriented AlN coatings deposited on Si substrates by radio frequency sputtering at different sputtering power densities, evaluating the coatings performance by nanoscratch. Authors indicate that friction and wear performance of the coatings is better than substrate at higher sputtering power density (~7.7 W cm^{-2}). Jatisukamto et al. [18] investigated surface roughness, specific wear and corrosion rate of AlN coatings deposited on AISI 410 steel by DC sputtering. From that study, they report an increase of hardness, decrease in corrosion rate and specific wear rate with respect to substrate that might be related to surface roughness. More recently, Choudhary et al. [19] tested the tribological performance of AlN coatings deposited on stainless steel on a reciprocating sliding PLINT machine where contact was formed by 6 mm diameter WC ball against a flat AlN coated counterface at ambient atmosphere. That study indicates that substrate biasing improved adhesion, hardness and wear resistance of AlN coatings. However, friction was higher for coatings deposited with a higher substrate bias and decreased with higher normal loads but a negligible change was observed at various sliding frequencies. From these previous studies it is clear that more detailed tribological studies are needed to elucidate how the main deposition parameters are related to friction and wear. Thus, in the present study, nanocrystalline AlN multilayer thin coatings were prepared by DC magnetron sputtering on AISI 52100 steel specimens to characterize their tribological response. The principal wear mechanisms presented under the test conditions were observed from micrographs of the wear track obtained with a scanning electron microscope (SEM).

2 EXPERIMENTAL PROCEDURE

In order to study the influence of nitrogen fraction (N_2 in mixed Ar + N_2 discharges) and the bilayer number (n) on the tribological behavior of multilayer $[Al/Al{-}N]_n$ coatings, multilayer coatings were synthetized at 35 and 65% N_2 for the Al–N layers and n = 35, 55 and 75. The coatings were deposited within a DC magnetron sputtering system, previously evacuated at $<3.8 \times 10^{-5}$ mbar, on polished AISI 52100 steel substrates located at 6 cm from aluminum target, which worked with a power density of 10.8 W/cm^2. The work pressure for both Al and AlN layers was automatically controlled by a system that includes mass flow controllers and a high-precision butterfly valve to maintain a pressure of 1.5×10^{-3} mbar. The aluminum layers were deposited in pure argon atmosphere whereas the Al–N layers were deposited in mixed Ar + N_2 discharges. The time deposition was 5 and 30 s for Al and Al–N layers, respectively, which produce different thicknesses (see Table 1). AISI52100 steel was selected as substrate since its tribological characteristics are well known. During deposition, substrates were maintained at ~200°C and –250 volts (substrate temperature and bias voltage, respectively). Before deposition, substrates were polished and cleaned by subsequent ultrasonic bath in acetone and ethanol for ten minutes each and finally dried with nitrogen gas. The r.m.s. roughness of the substrates and coatings under study (Table 1) were evaluated in an area of 1 × 1 μm with an atomic force microscope working in contact mode.

The structure of the coatings was assessed by X-ray diffraction (XRD) analysis in a Rigaku diffractometer model Dmax 2100 working with CoK_α radiation. Nanoindentation test were performed to evaluate the hardness of the coatings. The hardness was assessed from unloading portion of the load-displacement curves by using the Oliver and Pharr Method [20]. The nanoindentation system (UB1 Hysitron) was equipped with a Berkovich type diamond tip. Nine indentations per sample were performed at loads in the range of 9000 and 3000 μN to get the hardness dependence with indentation depth. Hardness and elastic modulus of the coating/substrate system data were fitted with the Korsunsky model [21] to determine the real hardness and the elastic modulus of the coatings without substrate influence.

Tribological experiments were conducted at nano and macro scales using an atomic force microscope and a pink-on-disk tribometer (CSM Instruments), respectively. For the experiment at the nanoscale, the counterpart was the tip of a cantilever beam coated with diamond-like carbon (Budgersensors 75 DLC). The test was carried out in a controlled atmosphere with relative humidity of <5% and temperature of ~23°C. Since the biggest uncertainly source during the friction force microscopy test is the quantification of the spring constant of the cantilever, this was obtained by finite element analysis following the procedure described by Espinoza-Beltrán et al. [22]. Such analysis allows the reproduction of the experimental resonance frequencies and real geometric characteristics of the cantilever. This procedure has been already used to characterize the tribological response of hard coat-

ings [23] and ceramics films [24]. In the case of tribological tests at the macroscale, balls of 6 mm diameter (AISI 52100) were used as pin, within an experimental environment with relative humidity of 60 ± 5% and temperature of ~23°C. The experiment was conducted with an applied force of 1 N on the ball, which produced an initial mean Hertzian pressure on samples of about 0.65 GPa. The sliding speed of the balls was 5 mm/s during 20 min. All tribological tests were carried out three times to confirm the results and the mean values are reported.

3 RESULTS AND DISCUSSION

3.1 Structural Analysis

XRD analysis (Fig. 1) reveals that multilayer $[Al/Al–N]_n$ coatings are formed by the AlN phase (indexed PDF#25-1133) with most of the grains having (002) crystallographic orientation, indicated by the intense peak at $2\theta = 36.04°$, independent of the bilayer number. As expected, coatings of Al–N layers at 35% N_2 exhibit, additional to AlN phase, a pure Al phase (indexed PDF#04-0787) with random crystallographic orientations (see Fig. 1a). However, the coatings with N_2 fraction of 65% in the Al–N layers are composed of an AlN phase only. The presence of the Al phase in the coatings at 35% N_2 indicates an effective switching from Al to AlN during the sputtering process. However, for the 65% N_2 fraction, the target suffered from nitridation [25] (or poisoning), which lead firstly to sputter AlN species instead of pure Al and this in turn, reduced the sputtering yield of pure metal and, as a consequence, an expected lower thickness, as can be seen in Table 1. This statement is in agreement with results observed by Petrov et al. [25], where they reported that during the sputtering process, the species present in the plasma are atoms, ions or molecules of the constituent elements with different contributions depending on the nitrogen fraction in the Ar + N_2 discharge. For high nitrogen fractions in the plasma, the N^{+2} ions become dominant resulting in a lower deposition rate due to difference in mass of the Ar+ ions with respect to N^{+2} ions.

A closer look to the main peak (002) in Figs. 1a, 1b reveals that, it does not have deviations related to diffraction at 36.04° of the (002) crystallographic orientation for the AlN phase. This suggests that internal stresses are relieved due to multilayer configuration. The crystallite size from this peak, determined by the Scherrer's formula, gives ~11 and ~10 nm for coatings with AlN layers of 35 and 65% N_2, respectively.

3.2 Mechanical Properties

As expected from XRD analysis, the hardness and the elastic modulus of the multilayer $[Al/AlN]_n$ coatings rise when N_2 fraction in the AlN layers increase from 35 to 65% (Fig. 2), because at 65% N_2 the coatings are composed of the AlN phase only, which is harder than Al phase. The mechanical properties of the coatings showed no dependence on the bilayer number, indicating that the mechanical properties of the coatings do not present significant changes when increasing the number of bilayers. The black line in Fig. 2 indicates the hardness and reduced elastic modulus for the substrate.

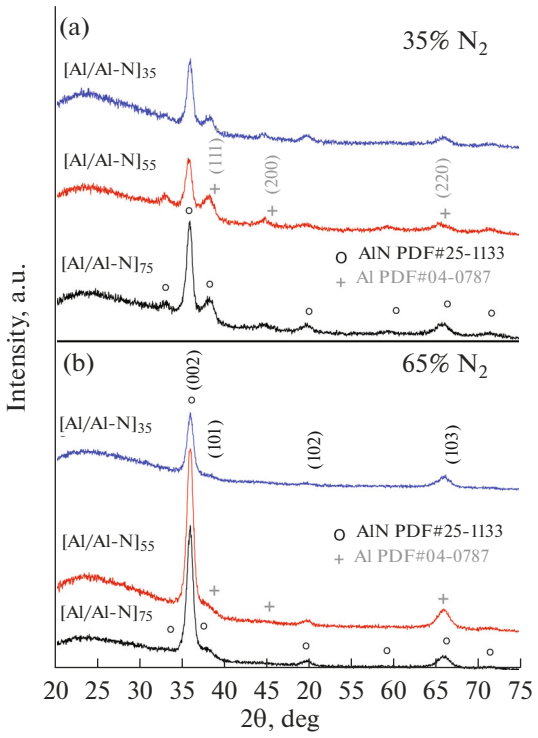

Fig. 1. XRD patterns of the $[Al/Al–N]_n$ coatings deposited at (a) 35 and (b) 65% N_2.

3.3 Tribological Results

3.3.1. Studies at the nanoscale. AFM topography images of the coatings under study revealed aggregates of size about 20 nm, independent of the N_2 content (Fig. 3). Experiments of friction force microscopy carried out on these surfaces are shown in Fig. 4, where the friction vs applied normal load plots indicate that coatings $[Al/AlN]_n$ have a lower friction coefficient than steel substrate. It is expected that at the nanoscale no correlation exist with bilayer number or N_2, since the top layer is the same (AlN) for all samples. The most important observation at this level was that all coatings presented a lower sliding friction resistance than steel substrate and the similarity of surface microstructures for all the samples. In order to elucidate the influence of n and N_2, macrotribological test were carried out and presented in the following section.

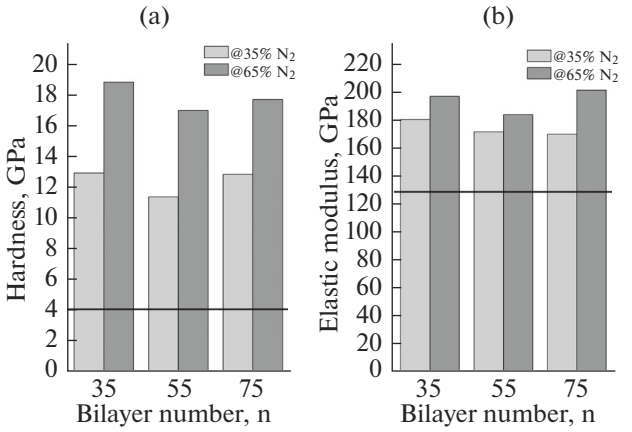

Fig. 2. Hardness and elastic modulus of $[Al/AlN]_n$ coatings. The black line corresponds to substrate's mechanical properties.

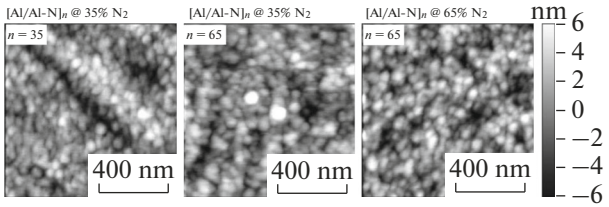

Fig. 3. AFM topographies of coatings at 35% (n = 35 and 65) and 65% (n = 65) N_2.

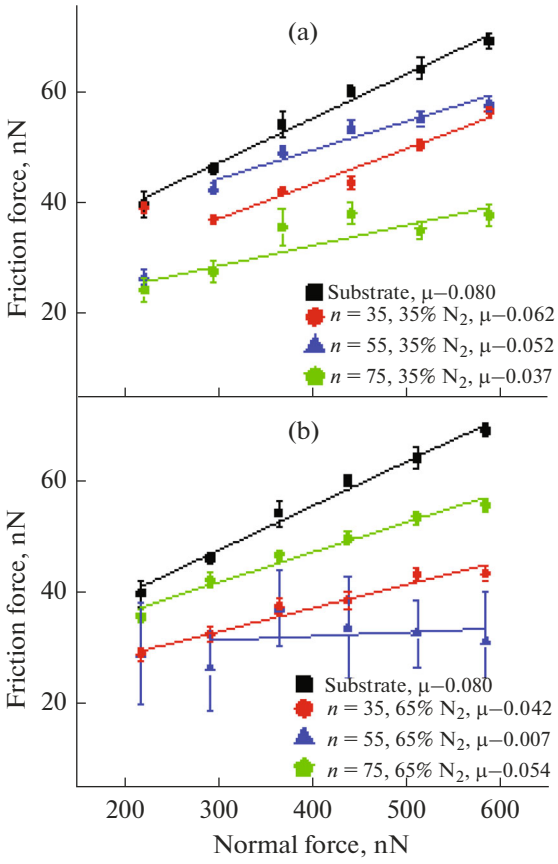

Fig. 4. Friction force microscopy results for all $[Al/Al-N]_n$ coatings.

3.3.2. Studies at the macroscale. For the tribological experiments at the macroscale, results shown in Fig. 5a indicate three frictional stages: (i) early stage, where friction depends exclusively on the surface asperities (running-in step); (ii) steady-state stage, where friction did not change appreciably over time and it is controlled by the coating-ball interaction but surface chemistry takes considerable importance (mechano-chemical interaction); (iii) final stage, which presented a faster friction rise and it was controlled by pure mechanical interaction. In this stage brittle fracture and ploughing effects were dominant, followed by adhesion as a consequence of welding and deformation of asperities.

The coatings with AlN layers at 35% N_2 present a lower μ than substrate and their steady-state response is maintained during the whole test for samples with 75 bilayers (see Fig. 5a). Interestingly, these coatings with n = 35 and n = 55 exhibited a low friction that raised after 500 s (approx. 8 min) reach a steady state but only the coating with n = 75 provides a low friction throughout the test. On the other hand, the brittle coatings (65% N_2) presented a μ higher than substrate in steady state conditions, which was longer than 35% N_2 coatings. Authors of this paper attribute the lower μ of coatings with Al–N layers of 35% N_2 to two main factors: firstly, the presences of layers with Al phase that allow the energy dissipation during the sliding test. These layers have a lower elastic modulus than AlN layers of 65% N_2, making possible to release the stresses and transfer them to the interior of Al layers. This is a similar effect to the one observed in coatings with gradient modulus [26, 27]. Secondly, the mechano-chemical interaction between the ball and the coatings, since the presence of Al phase allows the aluminum atoms to be exposed during the sliding test, being able to interact with the surrounding environment [28]. This can lead to the formation of a lubricious layer with low shear strength. Conversely, the coatings with 65% N_2 are brittle because their structure is controlled by AlN phase, which is hard but can be fractured by the mechanical stresses produced during sliding motion. The absence of that Al phase could inhibit the production of any lubricious layer.

The wear rate of the $[Al/Al–N]_n$ coatings is shown in Fig. 5b. The coatings with 35% N_2 have a higher wear rate than 65% N_2 coatings. This result indicates that although the coatings with 35% N_2 have lower hardness than 65% N_2 coatings their tribological behavior is better in terms of friction reduction but wear performance of 65% N_2 coatings is slightly better.

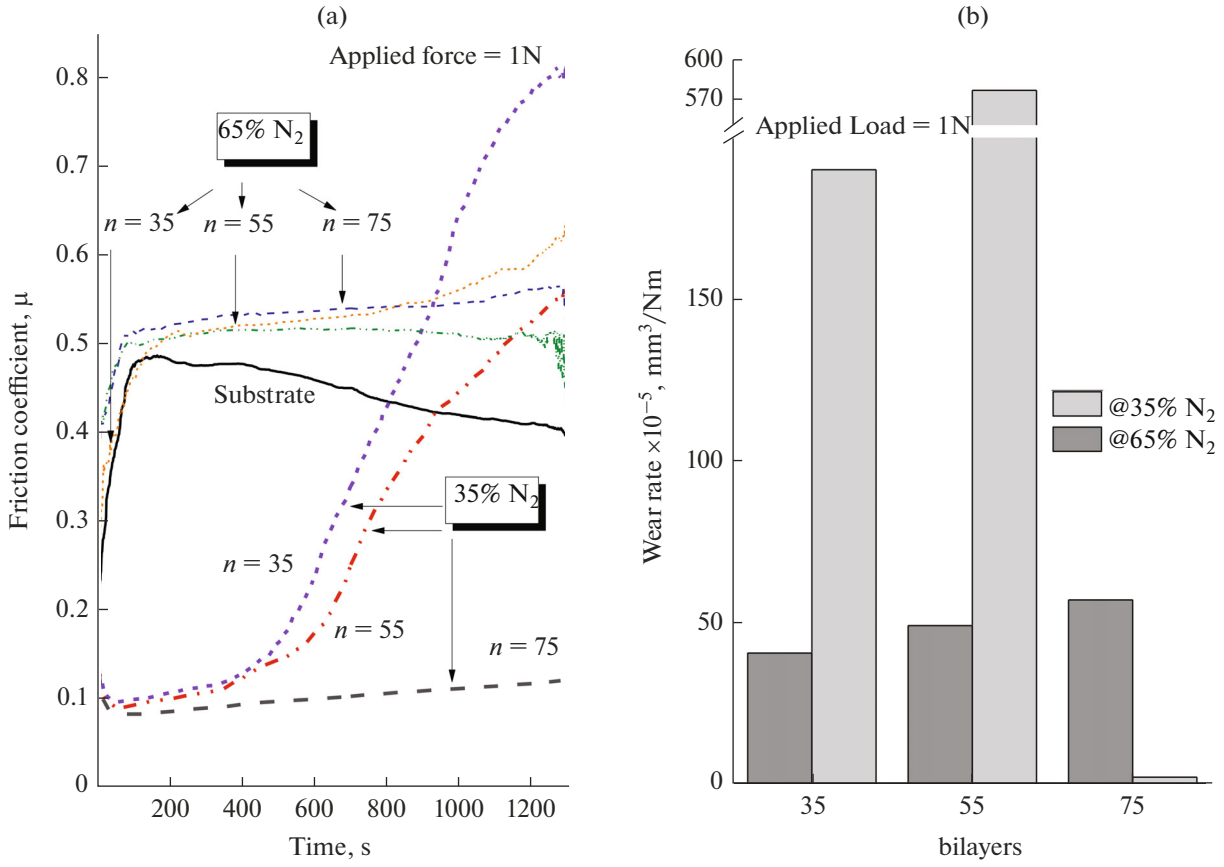

Fig. 5. (a) Friction coefficient as a function of sliding time and (b) wear rate of $[Al/Al–N]_n$ coatings.

Scanning electron micrographs on the wear track of the worn coatings and pin (right panels) were taken (Fig. 6) to elucidate the wear mechanism. Wear track from the substrate and pin were also analyzed and shown in Fig. 6. The dominant wear mechanism in 35% N_2 coatings was plastic flow and abrasive wear, while adhesive wear controlled the behavior of 65% N_2 coatings. The adhesive wear pattern correlates well with high friction coefficient observed in Fig. 6a. The higher wear rate observed in 35% N_2 coatings indicates that mechanical stresses are effectively transferred to Al layers, and atoms from these layers, exposed during sliding, interact with the surrounding environment. Otherwise, abrasive wear would produce higher wear values.

Friction and wear performance tests of AlN and other typical coatings like TiN, TiAlN and CrN deposited on steel samples by magnetron sputtering, carried out in past studies are presented in Table 2. Although there cannot be a direct comparison of those past studies with present tribological results from the authors of this paper, since tribological conditions are not exactly the same, comparison of this work with other studies indicate, in most cases, comparable friction coefficients as observed in references [19, 33, 34, 36].

Wear rate studies of multilayer coatings deposited by sputtering on steel are a few. Singh K. et al. reported wear rates of 40 to 55 × 10^{-5} ($mm^3\ N^{-1}\ m^{-1}$) for TiAlN on AISI 304 stainless steel against AISI52100 steel ball which are similar to wear rate results measured in this study for Al/AlN multilayer coatings of 65% N_2 against AISI52100 steel ball [34]. Choudhary R.K. et al. tested Al/AlN on AISI 304L stainless steel against WC ball and reported similar wear rate results [19]. Ou Y.X. et al. [36] reported higher wear rates for CrN/TiN multilayer coatings on AISI 304L stainless steel while Jatisukamto G. et al. [18] found lower wear rates on Al/AlN deposited on AISI 410 steel.

CONCLUSIONS

This study compares the mechanical and tribological properties of sputtered $[Al/Al–N]_n$ coatings with 35 and 65% N_2 on AISI52100 steel surfaces. Both 35 and 65% N_2 coatings were hard enough for industrial applications but interestingly, their friction performance was very different. Coatings with 35% N_2 presented a low and stable friction coefficient, whereas coatings with 65% N_2 exhibited higher friction coefficients than steel substrates. The main reason for the

Table 2. Tribological properties of selected coated surfaces from past studies

Coating	Substrate	Deposition method	Contact configuration	Tribological conditions	Tribological performance		Ref.
					wear rate $\times 10^{-5}$, $mm^3/N\ m$	μ	
Al/AlN multilayer	Steel AISI 52100	DC Sputtering	Ball-on-disk	5 mm/s, 1N, 65%N_2, 6 m	40–56	0.51–0.53	This Work
Al/AlN	Steel AISI 410	DC Sputtering	Ball-on-disk	20.8N, 2.44 m, 240 mm/s	4.6	–	[18]
Al/AlN	Steel AISI 304L	DC Sputtering	Reciprocating ball-on-flat	WC ball, 20 mm/s, 3N, 10 Hz, 180 s,	0.01–40	0.4–0.6	[19]
AlN–Cu–Mg	Al_2O_3	DC Plasma Nitriding	Pin-on-disk	Nitrided Al–Cu–Mg pin, 250 mm/s, 40N, 600 m	1.5	0.13	[29]
Al/AlN	Al	Laser-induced Plasma	Pin-on-disk	0.5N, 10 rpm, 50min	–	0.9	[30]
Al/AlN Multilayer	Si wafer	DC Sputtering	Ball-on-disk	1N, 100 rpm	–	0.15–0.25	[31]
AlN, CrN	Si wafer, Steel AISI D3	RF Sputtering	Pin-on-disk	0.5N, 1000 m	–	0.45 AlN, 0.35 CrN	[32]
Al/AlN multilayer	Si wafer	DC Sputtering	Ball-on-disk	100 rpm, 1N, stroke 6 mm,	–	0.15	[14]
VC/Ni multilayer	Steel M2	Non-Reactive Sputtering	Ball-on-disk	Al_2O_3 ball, 1N, 50 mm/s, 100 m	11	0.6	[33]
TiAlN	Steel AISI 304	Reactive DC Sputtering	Reciprocating ball-on-flat	3N, 15 Hz, 6 m AISI52100 balls, 10 mm/s, stroke 1 mm	40–55	0.5–0.6	[34]
Ti/TiN multilayer	Steel AISI 304	DC Sputtering	Ball-on-disk	Al_2O_3 balls 2000 cycles, 1N	2.5–23	0.19–0.22	[35]
CrN/TiN multi-layer	Steel AISI 304L	Unbalanced Sputtering	Reciprocating ball-on-flat	WC ball, 1N, 1 hr, 47.1 mm/s	75–110	0.41–0.88	[36]

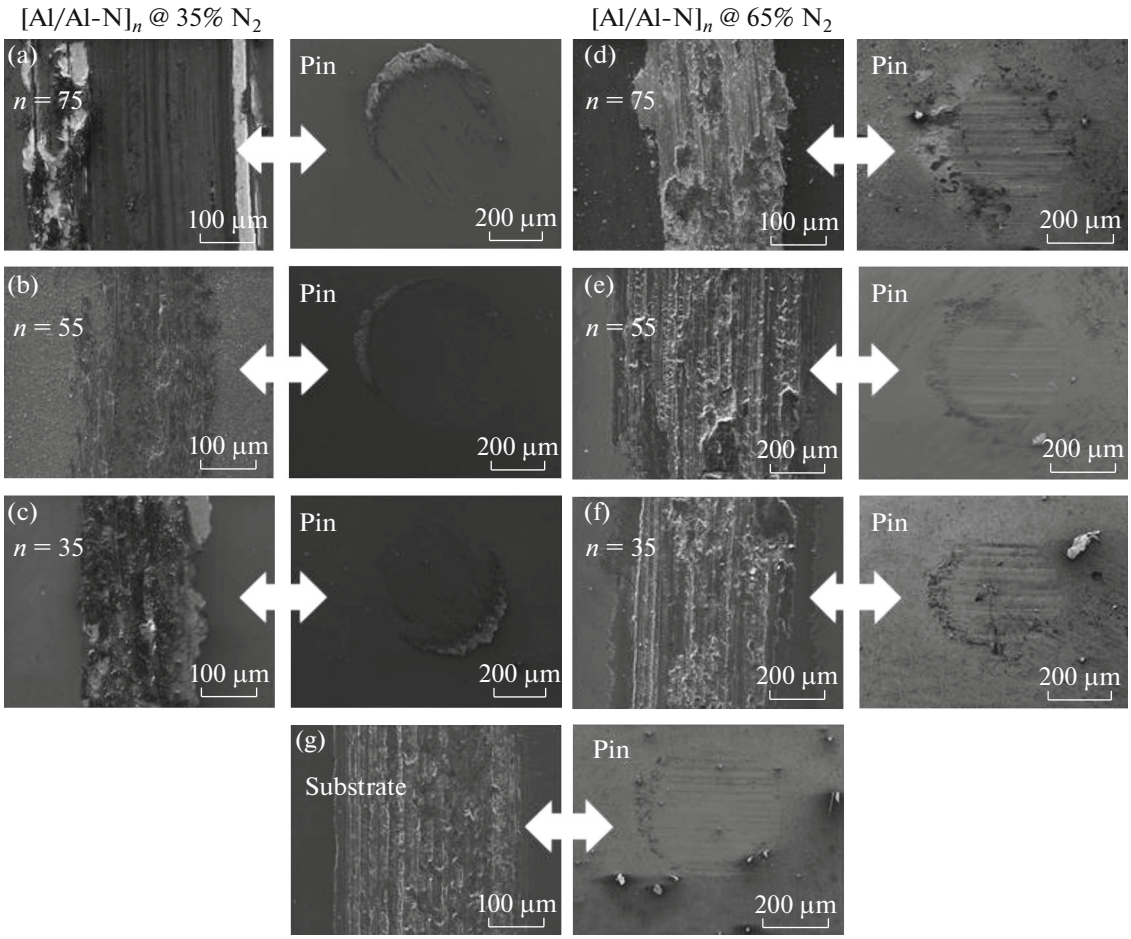

Fig. 6. SEM micrographs of disc and pin for n = 75, 55, 35 and N_2 of 35% (a–c) and 65% (d–f), (g) disc and pin from substrate.

high friction observed in coatings with 65% N_2 was the absence of an Al layer in the multilayer configuration. The Al layer was not present because during the sputtering process, the target experienced nitridation due to the high nitrogen concentration from the previous AlN layer. The wear mechanism for both 35 and 65% N_2 were different. For the first case, the wear is controlled by plastic flow and abrasive wear, while in the second case, is dominated by adhesive wear. These results show the important role that plays the Al phase in the tribological performance of Al-(N_2)-based multilayer coatings. Wear rates observed for coatings evaluated in this study are comparable to previous studies.

FUNDING

Authors wish to express their sincere thanks to the National Council for Science and Technology (CONACyT), Secretary of Public Education (SEP) and TecNM/Instituto Tecnologico de Oaxaca for the financial support under project 079901 to carry out the present work. FJFR thanks to CONACYT (Grant no. 2016-01-2488), and VIEP-BUAP 00559.

REFERENCES

1. Harper, J., Cuomo, J., and Hentzell, H., *Appl. Phys. Lett.,* 1983, vol. 43, p. 547.
2. Yoshida, S., Misawa, S., and Itoh, A., *Appl. Phys. Lett.,* 1975, vol. 26, p. 461.
3. Morita, M., Uesugui, N., Isogai, S., Tsubouchi, K., and Mikoshiba N., *Jpn. J. Appl. Phys.,* 1981, vol. 20, p. 17.
4. Rodriguez-Clements, R., Aspar, B., Azema, N., Armas, B., Combescure, C., Duran, J., and Figueras, A., *J. Cryst. Growth,* 1993, vol. 133, p. 59.
5. Yoshida, S., Misawa, S., Fujii, Y., Tanaka, S., Hirakawa, H., Gonda, S., and Itoh, A., *J. Vac. Sci. Technol.,* 1979, vol. 16, p. 990.
6. Miyauchi, M., Ishikawa, Y., and Shibata, N., *Jpn. Appl. Phys.,* 1992, vol. 31, p. L1714.
7. Calleja, E., Sánchez García, M.A., Monrroy, E., Sánchez, F.J., Muñoz, E., Sanz-Hervas, A., Villar, C.M., and Aguilar, M., *J. Appl. Phys.,* 1997, vol. 82, p. 4681.
8. Espinoza-Beltran, F.J., Bernal, R., Manzanares-Martinez, J., Garcia-Rodriguez, F.J., Perez Robles, J.F., Ramirez-Bon, R., Vorobiev, Y.V., and Gonzalez-Hernandez, J., *Mater. Sci. Forum,* 1998, vols. 287–288, p. 489.

9. Zhang, Y.J., Yan, P.X., Wu, Z.G., Xu, J.W., Zhang, W.W., Li, X., Liu, W.M. and Xue, Q.J., *J. Vac. Sci. Technol. A,* 2004, vol. 22, p. 2419.
10. Wei, G., Scharf, T.W., Zhou, J.N., Huang, F., Weaver, M.L., and Barnard, J.A., *Surf. Coat. Technol.,* 2001, vols. 146–147, p. 357.
11. Xu, J.H., Kamiko, M., Zhou, Y., Yamamoto, R., Li, G.Y., and Gu, M.Y., *J. Appl. Phys.,* 2001, vol. 89, p. 3674.
12. Pankov, V., Evstigneev, M., and Prince, R.H., *J. Appl. Phys.,* 2002, vol. 92, p. 4255.
13. Barshiliaa, H.C., Jainb, A., and Rajam, K.S., *Vacuum,* 2004, vol. 72, p. 241.
14. Wu, Z.G., Zhang, G.A., Wang, M.X., Fan, X.Y., Yan, P.X., and Xu, T., *Appl. Surf. Sci.,* 2006, vol. 253, p. 2733.
15. Wu, Z.G., Zhang, G.A., Wang, M.X., Fan, X.Y., and Yan, P.X., *Appl. Surf. Sci.,* 2007, vol. 253, p. 8835.
16. Subramanian, B., Ashok, K., and Jayachandran, M., *J. Appl. Electrochem.,* 2008, vol. 38, p. 619.
17. Yang, P., Jian, S., Wu, S., Lai, Y., Wang, Ch., and Chen, R., *Appl. Surf. Sci.,* 2009, vol. 255, p. 5984.
18. Jatisukamto, G., Malau, V., Ilman, M.N., and Iswanto, P.T., *Int. J. Eng. Technol. IJET-IJENS,* 2013, vol. 2, p. 129.
19. Choudhary, R.K., Mishra, S.C., Mishra, P., Limaye, P.K., and Singh, K., *J. Nucl. Mater.,* 2015, vol. 466, p. 69.
20. Oliver, G.M. and Pharr, W.C., *J. Mater. Res.,* 1992, vol. 7, p. 1564.
21. Korsunsky, A.M., McGurk, M.R., Bull, S.J., and Page, T.F., *Surf. Coat. Technol.,* 1998, vol. 99, p. 171.
22. Espinoza-Beltrán, F.J., Geng, K., Muñoz Saldaña, J., Rabe, U., Hirsekorn, S., and Arnold, W., *New J. Phys.,* 2009, vol. 11, p. 83034.
23. Flores-Ruiz, F.J., Enriquez-Flores, C.I., Chiñas-Castillo, F., and Espinoza-Beltrán, F.J., *Appl. Surf. Sci.,* 2014, vol. 314, p. 193.
24. Gervacio-Arciniega, J.J., Flores-Ruiz, F.J., Diliegros-Godines, C.J., Broitman, E., Enriquez-Flores, C.I., Espinoza-Beltrán, F.J., Siqueiros, J., and Cruz, M.P., *Appl. Surf. Sci.,* 2016, vol. 378, p. 157.
25. Petrov, I., Myers, A., Greene, J.E., and Abelson, J.R., *J. Vac. Sci. Technol., A,* 1994, vol. 12, p. 2846.
26. Zhang, Y., Sun, M.J., and Zhang, D., *Acta Biomater.,* 2012, vol. 8, p. 1101.
27. Rivera-Tello, C.D., Broitman, E., Flores-Ruiz, F.J., Jiménez, O., and Flores, M., *Tribol. Int.,* 2016, vol. 101, p. 194.
28. Sternitzke, M., *J. Am. Ceram. Soc.,* 1993, vol. 76, p. 2289.
29. Vissutipitukul, P. and Aizawa, T., *Wear,* 2005, vol. 259, p. 482.
30. Meneau, C., Andreazza, P., Andreazza-Vignolle, C., Goudeau, P., Villain, J.P., and Boulmer-Leborgne, C., *Surf. Coat. Technol.,* 1998, vols. 100–101, p. 12.
31. Zhang, G.A., Wu, Z.G., Wang, M.X., Fan, X.Y., Wang, J., and Yan, P.X., *Appl. Surf. Sci.,* 2007, vol. 253, p. 8835.
32. Cabrera, G., Torres, F., Caicedo, J.C., Amaya, C., De Sánchez, N.A., Mendoza, A., and Prieto, P., *Rev. Esc. Colomb. Ing.,* 2008 vol. 72, p. 71.
33. Fangfang, G.E., Xiaojun Zhou, Fanping Meng, Qunji Xue, and Feng Huang, *Tribol. Int.,* 2016, vol. 99, p. 140.
34. Singh, K., Limaye, P.K., Soni, N.L., Grover, A.K., Agrawal, R.G., and Suri, A.K., *Wear,* 2005, vol. 258, p. 1813.
35. Lackner, J.M., Major, L. and Kot, M., *Bull. Pol. Acad. Sci.: Tech. Sci.,* 2011, vol. 59, p. 343.
36. Ou, Y.X., Lin, J., Che, H.L., Sproul, W.D., Moore, J.J., and Lei, M.K., *Surf. Coat. Technol.,* 2015, vol. 276, p. 152.